# 1
# Basics of Corrosion Chemistry

*Norio Sato*

## 1.1
## Introduction

Metallic materials in practical use are normally exposed to corrosion in the atmospheric and aqueous environments. Metallic corrosion is one of the problems we have often encountered in our industrialized society; hence it has been studied comprehensively since the industrial revolution in the late eighteenth century. Modern corrosion science was set off in the early twentieth century with the local cell model proposed by Evans [1] and the corrosion potential model proved by Wagner and Traud [2]. The two models have joined into the modern electrochemical theory of corrosion, which describes metallic corrosion as a coupled electrochemical reaction consisting of anodic metal oxidation and cathodic oxidant reduction. The electrochemical theory is applicable not only to wet corrosion of metals at normal temperature but also to dry oxidation of metals at high temperature [3].

Metallic materials corrode in a variety of gaseous and aqueous environments. In this chapter, we restrict ourselves to the most common corrosion of metals in aqueous solution and in wet air in the atmosphere. In general, metallic corrosion produces in its initial stage soluble metal ions in water, and then, the metal ions develop into solid corrosion precipitates such as metal oxide and hydroxide. We will discuss the whole process of metallic corrosion from the basic electrochemical standpoint.

## 1.2
## Metallic Corrosion

### 1.2.1
### Basic Processes

The basic process of metallic corrosion in aqueous solution consists of the anodic dissolution of metals and the cathodic reduction of oxidants present in the solution:

$$M_M \rightarrow M_{aq}^{2+} + 2e_M^- \quad \text{anodic oxidation} \tag{1.1}$$

*Green Corrosion Chemistry and Engineering: Opportunities and Challenges,* First Edition.
Edited by Sanjay K. Sharma.

$$2Ox_{aq} + 2e_M^- \rightarrow 2Red(e_{redox}^-)_{aq} \quad \text{cathodic oxidation} \tag{1.2}$$

In the formulae, $M_M$ is the metal in the state of metallic bonding, $M_{aq}^{2+}$ is the hydrated metal ion in aqueous solution, $e_M^-$ is the electron in the metal, $Ox_{aq}$ is an oxidant, $Red(e_{redox}^-)_{aq}$ is a reductant, and $e_{redox}^-$ is the redox electron in the reductant. The overall corrosion reaction is then written as follows:

$$M_M + 2Ox_{aq} \rightarrow M_{aq}^{2+} + 2Red(e_{redox}^-)_{aq} \tag{1.3}$$

These reactions are charge-transfer processes that occur across the interface between the metal and the aqueous solution, hence they are dependent on the *interfacial potential* that essentially corresponds to what is called the *electrode potential* of metals in electrochemistry terms. In physics terms, the electrode potential represents the energy level of electrons, called the *Fermi level*, in an electrode immersed in electrolyte.

For normal metallic corrosion, in practice, the cathodic process is carried out by the reduction of hydrogen ions and/or the reduction of oxygen molecules in aqueous solution. These two cathodic reductions are *electron transfer* processes that occur across the metal–solution interface, whereas anodic metal dissolution is an *ion transfer* process across the interface.

### 1.2.2 Potential-pH Diagram

Thermodynamics shows that an electrode reaction is reversible at its equilibrium potential, where no net reaction current is observed. We then learn that the anodic reaction of metallic corrosion may occur only in the potential range more positive than its equilibrium potential and that the cathodic reaction of oxidant reduction may occur only in the potential range more negative than its equilibrium potential. Moreover, it is known that metallic corrosion in aqueous solution is dependent not only on the electrode potential but also on the acidity and basicity of the solution, that is, the solution pH.

The thermodynamic prediction of metallic corrosion was thus illustrated by Pourbaix [4] in the form of *potential–pH diagrams*, as shown for iron corrosion in Figure 1.1. The corrosion of metallic iron may occur in the potential–pH region where hydrated ferrous ions $Fe^{2+}$, ferric ions $Fe^{3+}$, and hydroxo-ferrous ions $Fe(OH)_3^-$ are stable. No iron corrosion occurs in the region where metallic iron is thermodynamically stable at relatively negative electrode potentials. In the regions where solid iron oxides and hydroxides are stable, no iron corrosion into water is expected to develop and the iron surface is covered with solid oxide films. In the diagram, we also see the equilibrium potentials of the hydrogen and oxygen electrode reactions. Atmospheric oxygen may cause iron corrosion in the potential range more negative than the oxygen equilibrium potential, $E_{O_2/H_2O}$, while hydrogen ions in aqueous solution may carry iron corrosion in the potential range more negative than the hydrogen equilibrium potential, $E_{H^+/H_2O}$.

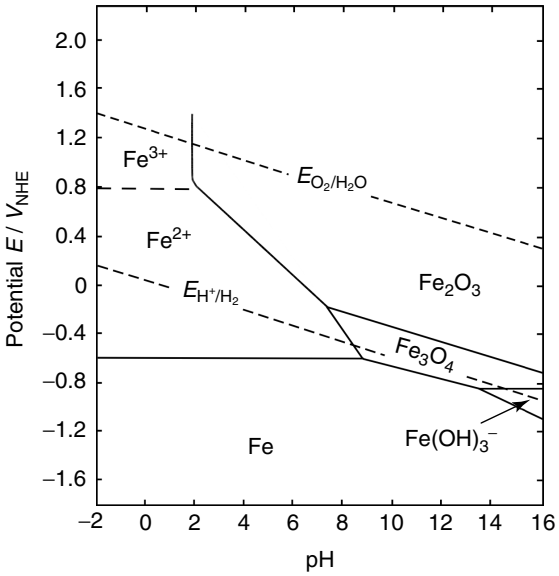


**Figure 1.1** Potential–pH diagram for iron corrosion in water at room temperature. $E_{O_2/H_2O}$ is the equilibrium potential for the oxygen electrode reaction, $E_{H^+/H_2O}$ is the equilibrium potential for the hydrogen electrode reaction, and $V_{NHE}$ is volt on the normal hydrogen electrode scale [4].

We note that the potential–pH diagram normally assumes metallic corrosion in pure water containing no foreign solutes. The presence of foreign solutes in aqueous solution may affect the corrosion and anticorrosion regions in the potential–pH diagram. We see in the literature a number of potential–pH diagrams for metallic corrosion in the presence of foreign solutes such as chloride and sulfides [4, 5].

### 1.2.3 Corrosion Potential

An electrode of metal corroding in aqueous solution has an electrode potential, which is called the *corrosion potential*. As a matter of course, the corrosion potential stands somewhere in the range between the equilibrium potential of the anodic metal dissolution and that of the cathodic oxidant reduction. It comes from the kinetics of metallic corrosion that at the corrosion potential, the anodic oxidation current of the metal dissolution is equal to the cathodic reduction current of the oxidant. The corrosion kinetics is usually described by the electrode potential versus reaction current curves of both the anodic oxidation and the cathodic reduction, as schematically shown in Figure 1.2, which electrochemists call the *polarization curves* of corrosion reactions. We see in Figure 1.2 that the intersecting point of the anodic and cathodic polarization curves represents the state of corrosion, namely, the corrosion potential and the corrosion current. We then realize that the corrosion

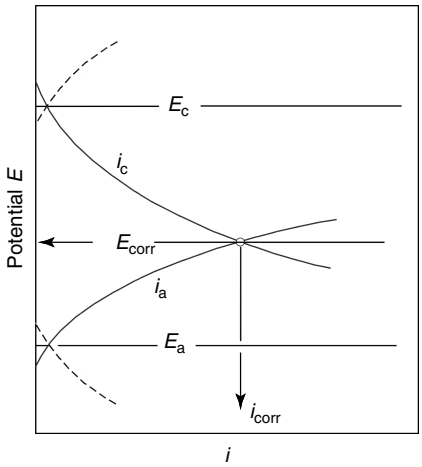


**Figure 1.2** Conceptual potential–current curves of anodic and cathodic reactions for metallic corrosion; $i_a$ is the anodic reaction current, $i_c$ is the cathodic reaction current, $i_{corr}$ is the corrosion current, $E_a$ is the equilibrium potential of the anodic reaction, $E_c$ is the equilibrium potential of the cathodic reaction, and $E_{corr}$ is the corrosion potential.

potential is determined by both the anodic and cathodic polarization curves of the corrosion reactions.

The corrosion rate of metals may be controlled by either the anodic or the cathodic reaction. In most cases of metallic corrosion, the cathodic hydrogen ion reduction controls the rate of metallic corrosion in acidic solution, while in neutral solution, the cathodic oxygen reduction preferentially controls the corrosion rate. If the corrosion potential comes out far away from the equilibrium potential of the cathodic reaction, the corrosion rate will be controlled by the cathodic reaction. In practice, we see that metallic corrosion is often controlled by the oxygen diffusion toward the corroding metal surface, in which the corrosion potential is far more negative than the oxygen equilibrium potential.

### 1.2.4 Anodic Metal Dissolution

Electrochemical kinetics gives the reaction current, $i_a$, of anodic metal dissolution as an exponential function of the electrode potential, $E$, of the metal as follows:

$$i_a = K_a \exp\left(\frac{\alpha_a E}{kT}\right) \tag{1.4}$$

In Eq. (1.4), $K_a$ and $\alpha_a$ are parameters. The anodic dissolution current of metallic iron, in fact, increases exponentially with the anodic electrode potential in acid solution as shown in Figure 1.3 [6].

Anodic metal dissolution depends not only on the electrode potential but also on the acidity and foreign solutes present in the aqueous solution. It is a received

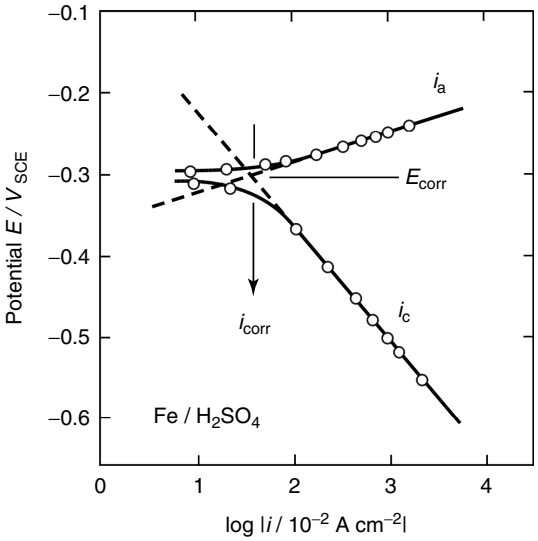


**Figure 1.3** Potential–current curves for corroding iron in sulfuric acid solution at pH 1.7 at 25 °C; $V_{SCE}$ is the volt on the saturated calomel electrode scale [6].

understanding that the anodic dissolution current of metallic iron depends on the concentration of hydroxide ions in the solution. Hydrated anions other than hydroxide ions also have some effects on the anodic metal dissolution. Hydrated hydroxide ions are found to accelerate the anodic iron dissolution in weekly acidic solution; whereas they decelerate (hydrated hydrogen ions accelerate) the iron dissolution in strongly acidic solution [7]. Furthermore, in acidic solution, hydrated chloride ions accelerate the anodic iron dissolution in relatively concentrated chloride solution, while they inhibit the iron dissolution in relatively dilute chloride solution [7]. These facts suggest that anions of different sorts compete with one another in participating in the process of anodic metal dissolution probably through their adsorption on the metal surface forming activated intermediates, such as $FeOH^{+}_{ad}$ and $FeCl^{+}_{ad}$, which will determine the metal dissolution rate [7].

It is worth noting that, in general, the surface of metal is *soft acid* in the Lewis acid–base concept [8] and tends to adsorb ions and molecules of *soft base*, forming covalent bonds between the metal surface and the adsorbates. It is also noteworthy that as the anodic metal potential increases in the more positive direction, the Lewis acidity of the metal surface may gradually turn from *soft acid* to *hard acid*. The anions of *soft base* adsorbed in the range of less positive potentials are then replaced in the range of more positive potentials by anions of *hard base* such as hydroxide ions and water molecules. In general, iodide ions $I^{-}$, sulfide ions $S^{-}$, and thiocyanate ions $SCN^{-}$ are the *soft bases*, while hydroxide ions $OH^{-}$, fluoride ions $F^{-}$, chloride ions $Cl^{-}$, phosphate ions $PO_4^{3-}$, sulfate ions $SO_4^{2-}$, and chromate

ions $CrO_4^{2-}$ are the *hard bases*. Bromide ions $Br^-$ and sulfurous ions $SO_3^{2-}$ stand somewhere between the *soft base* and the *hard base*.

### 1.2.5 Cathodic Oxidant Reduction

The cathodic current, $i_c$, of oxidant reduction is also an exponential function of the electrode potential, $E$, of the metal as follows:

$$i_c = K_c \exp\left(\frac{-\alpha_c E}{kT}\right) \tag{1.5}$$

For metallic iron in acid solution, where the hydrogen ion reduction carries the cathodic reaction of corrosion, the cathodic current increases exponentially with increasing cathodic electrode potential in the more negative direction as shown in Figure 1.3.

The cathodic reaction for usual metallic corrosion is carried by the hydrogen reaction and/or the oxygen reaction. For the hydrogen reaction, there are two cathodic processes that produce hydrogen gas at metal electrodes: one is the reduction of hydrogen ions and the other is the reduction of water molecules.

$$2H_{aq}^+ + 2e_M^- \rightarrow H_{2,gas} \tag{1.6}$$

$$2H_2O + 2e_M^- \rightarrow H_{2,gas} + 2OH_{aq}^- \tag{1.7}$$

Hydrogen ion reduction preferentially occurs in acidic solution, and its reaction current increases with increasing hydrogen ion concentration. Water molecule reduction occurs in weakly acidic and neutral solutions. The cathodic polarization curves (potential–current curves) of these two reactions are different from each other. The cathodic current of hydrogen ion reduction increases with increasing cathodic electrode potential until it reaches a limiting current of hydrogen ion diffusion toward the metal surface, and beyond a certain cathodic potential, the cathodic current of water molecule reduction emerges and increases with the cathodic electrode potential [9].

For oxygen reduction, similarly, there are two cathodic processes: one involves hydrogen ions and the other requires water molecules.

$$O_{2,gas} + 4H_{aq}^+ + 4e_M^- \rightarrow 2H_2O \tag{1.8}$$

$$O_{2,gas} + 2H_2O + 4e_M^- \rightarrow 4OH_{aq}^- \tag{1.9}$$

The oxygen reduction involving hydrogen ions takes place preferentially in acidic solution with the reaction current limited not only by the oxygen diffusion but also by the hydrogen ion diffusion toward the metal surface; whereas the oxygen reduction requiring water molecules develops in neutral and alkaline solutions and its reaction current is limited by the oxygen diffusion [9]. It is most likely in practical environments that the corrosion of metals is controlled by the diffusion of oxygen toward the surface of corroding metals.

## 1.3
## Metallic Passivity

### 1.3.1
### Passivity of Metals

Metallic passivity was discovered in 1790 by Keir [10], who found that metallic iron violently corroding in the active state in concentrated nitric acid solution suddenly turned into the passive state where almost no corrosion was observed. It was not until 1960s that we confirmed the presence of an oxide film several nanometers thick on the surface of passivated metals [11]. Latest overviews on metallic passivity may be referred to in the literature of corrosion science [12].

We illustrate metallic passivity with the potential–current curve of anodic metal dissolution for metallic iron, nickel, and chromium in acid solution as shown in Figure 1.4. Anodic metal passivation occurs at a certain potential, called the *passivation potential*, $E_P$, beyond which the anodic current of metal dissolution drastically decreases to a negligible level. It is an observed fact that the passivation potential depends on the solution acidity, lineally shifting in the more positive direction with decreasing solution pH. This fact thermodynamically suggests that metallic passivity is caused by the formation of an oxide film on the metal, which is extremely thin and invisible to the naked eye.

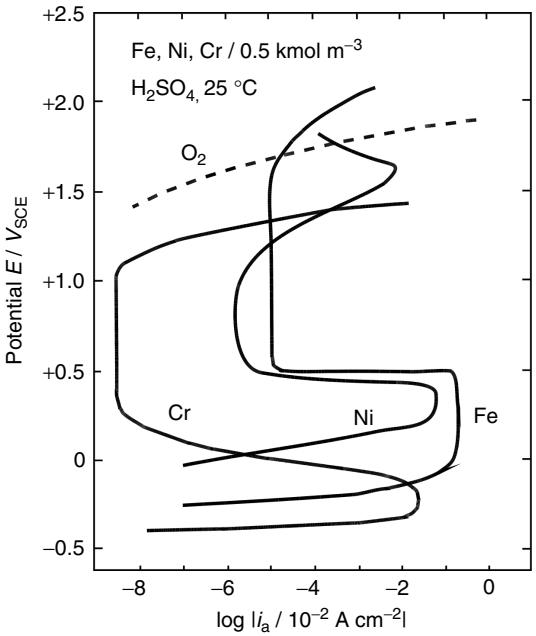


**Figure 1.4** Potential–current curves for anodic dissolution of iron Fe, nickel Ni, and chromium Cr in 0.5 mol $m^{-3}$ sulfuric acid solution at 25 °C; $O_2$ is anodic oxygen evolution current.

In the potential range of passivity, a nanometer-thin oxide film is formed on the metal, which is called the *passive film*. The film grows in thickness with increasing anodic potential at the rate of 1–3 nm $V^{-1}$ equivalent to an electric field of $10^6$–$10^7$ V $cm^{-1}$ across the film [13]. For most of the iron group metals, the passive film is less than several nanometers in thickness in the potential region where it is stable. For some metals such as aluminum and titanium, the passive oxide film can be made thick up to several hundred nanometers by increasing anodic potential; the thick oxide is frequently called the *anodic oxide*.

In the potential range where the passive state is stable, as shown in Figure 1.4, the metal anode normally holds an extremely small, potential-independent metal dissolution current, which is equivalent to the dissolution rate of the passive film itself. We see that the anodic metal dissolution current in the passive state is controlled by the dissolution rate of the passive film. The potential-independent dissolution of passive metals results from the fact that the interfacial potential between the passive oxide film and the solution, which controls the film dissolution rate, remains constant independent of the anodic potential, although depending on the solution pH [12, 14, 15].

For some metals, the passive state turns beyond a certain potential to be what is called the *transpassive* state, where the anodic dissolution current for the most part increases exponentially with the anodic potential as shown in Figure 1.4. The anodic metal dissolution in the transpassive state is thus controlled by the potential-dependent dissolution of the transpassive film. In the transpassive potential range, the interfacial potential between the film and the solution is not constant but depends on the anodic potential of the metal. The passive film is stable as long as the Fermi level (the electrode potential) of the metal anode is within the band gap of electron energy between the conduction and valence bands of the film, a situation which realizes the nonmetallic nature of the interface and hence makes the interfacial potential independent of the metal potential [12, 14, 15]. As the anodic potential increases, the Fermi level finally reaches the valence band edge of the film at the film–solution interface and the quasi-metallization (electronic degeneracy) is realized at the same. The film–solution interfacial potential, hence, turns to be dependent on the anodic metal potential, and as a result, potential-dependent transpassive dissolution occurs beyond the transpassivation potential, $E_{TP}$.

Let us see the anodic metal dissolution of iron, nickel, and chromium in acid solution as shown in Figure 1.4. While going into solution as hydrated ferrous ions in the active state, metallic iron in the passive state dissolves in the form of hydrated ferric ions, indicating that the passive film is ferric oxide, $Fe_2O_3$.

$$2Fe + 3H_2O \rightarrow Fe_2O_3 + 6H^+_{aq} + 6e^-_M \quad \text{passive film formation} \tag{1.10}$$

$$Fe_2O_3 + 6H^+_{aq} \rightarrow 2Fe^{3+}_{aq} + 3H_2O \quad \text{passive film dissolution} \tag{1.11}$$

These two reactions proceed simultaneously, maintaining the passive film at a steady thickness, which increases with increasing anodic potential.

Anodic nickel dissolution produces divalent nickel ions both in the active and passive states, implying that the passive film is divalent nickel oxide.

$$Ni + H_2O \rightarrow NiO + 2H^+_{aq} + e^-_M \quad \text{passive film formation} \tag{1.12}$$

$$NiO + 2H^+_{aq} \rightarrow Ni^{2+}_{aq} + H_2O \quad \text{passive film dissolution} \tag{1.13}$$

In the transpassive state, as mentioned earlier, the film dissolution rate is potential dependent in contrast to the passive state in which it is potential independent. Since the dissolution current increases with the anodic potential, the thickness of the transpassive film seems to decrease with the anodic potential in the steady state. Beyond the transpassive potential range of nickel, the transpassive divalent oxide film is assumed to change near the oxygen evolution potential into a trivalent oxide film causing a decrease in the anodic nickel dissolution current [11].

For chromium, the anodic dissolution produces divalent chromium ions in the active state and the passivation occurs forming an extremely thin, trivalent chromium oxide film on the metal surface.

$$2Cr + 3H_2O \rightarrow Cr_2O_3 + 6H^+_{aq} + 6e^-_M \quad \text{passive film formation} \tag{1.14}$$

$$Cr_2O_3 + 6H^+_{aq} \rightarrow 2Cr^{3+}_{aq} + 3H_2O \quad \text{passive film dissolution} \tag{1.15}$$

$$Cr_2O_3 + 5H_2O + 6e^-_M \rightarrow 2{CrO_{4,aq}}^{2-} + 10H^+_{aq} \quad \text{transpassive film dissolution} \tag{1.16}$$

The transpassive dissolution of metallic chromium is the oxidative dissolution of trivalent chromic oxide into soluble hexavalent chromate ions in acidic solution; hence the anodic transpassive dissolution proceeds through the formation of a chromic oxide film on the metal surface.

### 1.3.2 Passivation of Metals

A metallic electrode may be made passive if its corrosion potential is held in the potential range of passivity. The corrosion potential is determined, as mentioned earlier, by both the anodic metal dissolution current and the cathodic oxidant reduction current. As shown in Figure 1.5, the corrosion potential remains in the active state as long as the cathodic current is less than the maximum current of anodic metal dissolution; whereas it goes to the passive potential range when the cathodic current exceeds the anodic dissolution current. An unstable passive state arises if the cathodic potential–current curve crosses the anodic potential–current curve at two potentials, one in the passive state and the other in the active state. A metallic electrode in the unstable passive state, once its passivity breaks down, never repassivates because the cathodic current of oxidant reduction is insufficient in magnitude for the activated metal to clear its anodic dissolution current peak.

It has been observed that metallic nickel corrodes in acidic solution but passivates in basic solution: the transition from the active corrosion to passivation occurs at pH 6 in sulfate solution [16]. The corrosion of nickel in weakly acidic and neutral solutions is controlled by cathodic oxygen reduction whose current is limited by

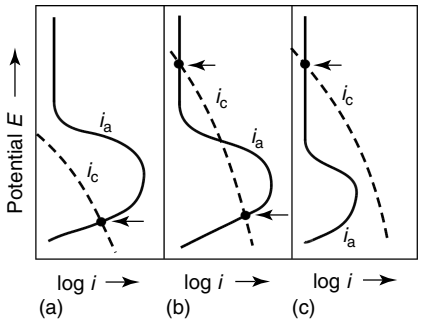


**Figure 1.5** Passivation of metals and its stability. (a) Active corrosion, (b) unstable passivity, (c) stable passivity; $i_a$ is the anodic current and $i_c$ is the cathodic current.

the oxygen diffusion toward the metal surface. The nickel dissolution current peak in the active state decreases with increasing solution pH and becomes less than the cathodic oxygen diffusion current beyond pH 6. Consequently, metallic nickel passivates in a solution more basic than pH 6, which is called the *passivation* pH of nickel.

Let us see the oxidizing agent of nitrite ion $NO_2^-$ that provides a cathodic reaction for the corrosion and passivation of metallic iron in weakly acidic and neutral solutions.

$$NO_{2,aq}^- + 5H_2O + 6e_M^- \rightarrow NH_3 + 7OH_{aq}^- \quad \text{cathodic reaction} \tag{1.17}$$

$$2Fe \rightarrow 2Fe_{aq}^{2+} + 4e_M^-$$

$$2Fe + 3H_2O \rightarrow Fe_2O_3 + 6H_{aq}^+ + 6e_M^- \quad \text{anodic reaction} \tag{1.18}$$

Metallic iron remains in the active state if the cathodic reaction current is insufficient for the metal to passivate; whereas it turns out to be passive forming a surface film of ferric oxide if the cathodic reaction current surmounts the metal dissolution current peak. Owing to its relatively more-positive redox potential and its greater reaction current, an amount of nitrite salt readily brings metallic iron into the passive state, and thus, it provides an effective passivating reagent for iron and steel.

It is also noted that chromate ions, $CrO_4^{2-}$, oxidize metallic iron to form a passive film of chromic–ferric mixed oxides on the metal surface.

$$CrO_{4,aq}{}^{2-} + 10H_2O + 6e_M^- \rightarrow Cr_2O_3 + 5H_2O \quad \text{cathodic reaction} \tag{1.19}$$

$$2Fe + 3H_2O \rightarrow Fe_2O_3 + 6H_{aq}^+ + 6e_M^- \quad \text{anodic reaction} \tag{1.20}$$

Chromate is one of the strongest oxidants to passivate metallic materials. In the same way, molybdate and tungstate may also make metallic iron passive, although their oxidizing capacity may not always be sufficient.

### 1.3.3 Passive Films

The passive oxide film on metals is very thin, of the order of several nanometers, and hence, sensitive to the environment in which it is formed. In the formation and growth processes of the film, the oxide ions migrate from the solution across the film to the metal–oxide interface forming an inner oxide layer, while the metal ions migrate from the metal to the oxide–solution interface to react with adsorbed water molecules and solute anions forming an outer oxide layer, which occasionally incorporates anions other than oxide ions into itself. The anion incorporation occurs only when the migrating metal ions react with the adsorbed anions. The ratio of the thickness of the outer anion-incorporating layer to the overall layer is expressed by the transport number, $\tau_M$, of the metal ion migration during the film growth. The transport number was found to be $\tau_M = 0.7–0.8$ for an anodic oxide film 65 nm thick formed on aluminum in phosphate solution [17].

The passive film is mostly amorphous, but as the film grows thicker, it may turn to be crystalline. For the passivity of metallic titanium in sulfuric acid solution, the passive film appears to change from amorphous to crystalline beyond the anodic potential of about 8 V, probably because of the internal stress created in the film [18]. The passive film is either an insulator or a semiconductor. For metallic iron, titanium, tin, niobium, and tungsten, the passive film is an n-type semiconductor with donors in high concentration. Some metals such as metallic nickel, chromium, and copper make the passive film a p-type semiconductor oxide. The passive films on metallic aluminum, tantalum, and hafnium are insulator oxides.

We may classify the passive oxide films into two categories: the network former (glass former) and the the network modifier [19]. The network former, which includes metallic silicon, aluminum, titanium, zirconium, and molybdenum, normally forms a single-layered oxide film. On the other hand, the network modifier, which includes metallic iron, nickel, cobalt, and copper, tends to form a multilayered oxide film, such as a cobalt oxide film, consisting of an inner divalent oxide layer and an outer trivalent oxide layer ($Co/CoO/Co_2O_3$). High-valence metal oxides normally appear to be more corrosion resistive than low-valence metal oxides. The anodic formation of network-forming oxides is most likely carried through the inward oxide ion migration to the metal–oxide interface and hence will probably produce a dehydrated compact film containing no foreign anions other than oxide ions; whereas, network-modifying oxides appear to grow through the outward metal ion migration to the oxide–solution interface forming a more or less defective film occasionally containing foreign anions.

It is worth noting that since the passive film is so extremely thin, electrons easily transfer across the film by the quantum mechanical electron tunneling mechanism, irrespective of whether the passive film is an insulator or a semiconductor. By contrast, however, no ionic tunneling is allowed to occur across the passive film. The passive film thus constitutes a barrier layer to ion transfer but not to electron transfer. Any redox electron transfer reaction is therefore allowed to occur on the passive film-covered metal surface just like on the metal surface without any film.

### 1.3.4
### Chloride-Breakdown of Passive Films

The passive film on metals may break down in the presence of aggressive ions, such as chloride ions, in solution, and the breakdown site may trigger a localized corrosion of the underlying metals. The chloride-breakdown of passive films, in general, occurs beyond a certain potential, which we call the *film breakdown potential*, $E_b$. Either repassivation or pitting corrosion then follows at the breakdown site, as schematically shown in Figure 1.6. Pitting corrosion is also characterized by a threshold potential, called the *pitting potential*, $E_{pit}$, above which pitting grows but below which pitting ceases to occur. These two potentials, $E_b$ and $E_{pit}$, are influenced by the concentrations of chloride ions and hydrogen ions in the solution.

There is a marginal chloride concentration below which no film breakdown occurs. For chloride-breakdown of the passive film on metallic iron, the concentration of chloride ions required for the film breakdown depends on the film thickness, defects in the film, the electric field intensity in the film, and pH of the solution [20]. It is also found that the passive film locally dissolves and thins down before the underlying metal begins pitting at the film breakdown site [21, 22]. It is then likely that the film breakdown results not from a mechanical rupture but from a localized mode of film dissolution because of the adsorption of chloride ions.

It is frequently seen that the passive film preferentially breaks down at the sites of crystal grain boundaries, nonmetallic inclusions, and flaws on the metal surface. For stainless steels, the passivity breakdown and pit initiation most likely occur at the site of nonmetallic inclusions of MnS. It is noted that any localized phenomena are nondeterministic and in general, somehow stochastic. Chloride-breakdown of passive films on stainless steels was found to come out in accordance with a stochastic distribution [23, 24].

The pitting potential, $E_{pit}$, at which pitting begins to grow, arises at a potential either more positive (more anodic) or less positive (more cathodic) than the film

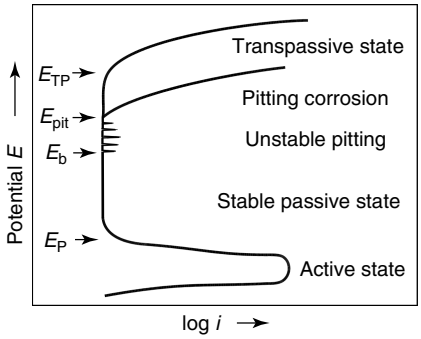


**Figure 1.6** Schematic potential–current curves for metallic passivation, passive-film breakdown, pitting dissolution, and transpassivation; $E_b$ is the film breakdown potential, $E_{pit}$ is the pitting potential, $E_P$ is the passivation potential, and $E_{TP}$ is the transpassivation potential.

breakdown potential, $E_b$. When the film breakdown potential is less-positive than the pitting potential, the breakdown site repassivates, as we observe for some stainless steels in acid solution [25]. On the other hand, pitting corrosion follows film breakdown when the film breakdown potential emerges more positive than the pitting potential, as we observe for metallic iron in acid solution [22].

For the mechanism of chloride-breakdown of passive films, one of the currently prevailing models is the ionic point defect model that assumes injection of metal ion vacancies into the passive film at the adsorption site of chloride ions. The ionic point defects thus injected migrate to and accumulate at the metal–film interface, finally creating a void there to break the film down [26]. Another model is the electronic point defect model that assumes injection of an electronic defect level localized at the film–solution interface. The electronic interfacial state thus injected causes local quasi-metallization at the adsorption site of chloride ions, finally resulting in a local mode of film dissolution [14, 15, 27]. There have also been several chemical models for passivity breakdown, which more or less assume the formation of a soluble chloride complex at the chloride adsorption site.

We note at the end that the passivity breakdown is different from the pitting that follows: the former is a process associated with the passive film itself, whereas the underlying metal is responsible for the latter.

## 1.4 Localized Corrosion

### 1.4.1 Pitting Corrosion

Pitting corrosion of metals in general occurs in the potential range more positive than the *pitting potential*, $E_{pit}$ [28]. For usual stainless steel in 1 mol $dm^{-3}$ sodium chloride solution, the pitting potential arises around +0.3 V on the normal hydrogen electrode (NHE) scale [29]. Once metallic pitting sets in, the anodic metal dissolution current increases with the anodic potential as schematically shown in Figure 1.6. The pit initially grows in a semispherical shape with the pit solution that acidifies and concentrates in soluble metal salts. For 304 stainless steels in neutral chloride media at pH = 6 ~ 8, the local pH in the pit falls down to pH = 1 ~ 2 [29]. The kinetics of pit dissolution appears to be different from that of metal dissolution in the active state. The pitting dissolution current density, $i_{pit}$, is given by an exponential function of the anodic potential, $E$.

$$E = a + b \log i_{pit} \tag{1.21}$$

In acid solution, the coefficient $b$ (Tafel constant) is 0.20 V for metallic iron [30] and 0.30 V for stainless steel [29]. These Tafel constants are much greater than those (0.03 ~ 0.1 V) normally observed for anodic metal dissolution in the active state. The metal dissolution in the pit proceeds in an acidified, concentrated salt

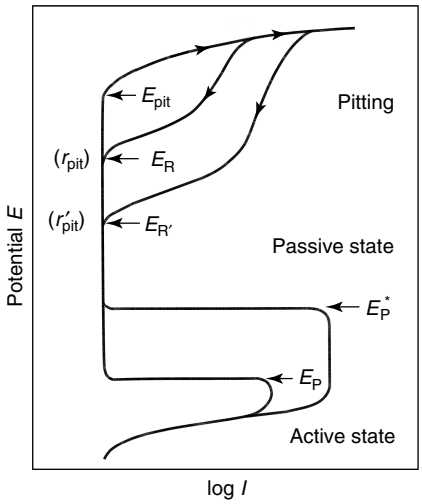


**Figure 1.7** Schematic potential–current curves for metallic pitting dissolution, and pit repassivation; $r_{pit}$ is the pit radius ($r'_{pit} > r_{pit}$), $E_P^*$ is the passivation–depassivation potential for the critical pit solution, and $E_P$ is the passivation–depassivation potential for the solution outside the pit.

solution with an electropolishing mode of dissolution, which is different from the usual mode of metal dissolution in the potential range of the active state.

As the electrode potential of pitting metal is made more negative, we come to a certain potential at which the pitting metal dissolution ceases to occur, resulting in repassivation of the pit, a certain potential which we call the *pit-repassivation potential*, $E_R$. The pit-repassivation potential is found to move more negative with increasing pit size, as schematically shown in Figure 1.7. We may then assume that a pit embryo takes a certain critical size at the pitting potential, $E_{pit}$, at which the pitting starts to occur. For stainless steel in acidic chloride solution, the smallest pit size for the initiation of pitting was estimated at 0.01–0.02 mm [29].

From the kinetics of pitting dissolution and mass transport in a semispherical pit, it is deduced that the pit-repassivation potential $E_R$ is a logarithmic function of pit radius $r_{pit}$ [29].

$$E_R = a + b \log r_{pit} \tag{1.22}$$

We in fact observe that a logarithmic dependence of the pit-repassivation potential on the pit radius is held for stainless steel in acid solution [31].

It appears that the pitting mode of metal dissolution requires highly concentrated acidic chloride in the pit solution, whose chloride ions must be more concentrated than a certain critical value, $c^*_{Cl^-}$. For usual stainless steel in acid solution, the critical chloride concentration was estimated to be $c^*_{Cl^-} = 1.8\ \mathrm{kmol\,m^{-3}}$ [29]. The pit solution is also highly acidified to keep running a polishing mode of pitting dissolution and preventing the pit from repassivation at potentials more positive than $E_R$. The critical chloride concentration, $c^*_{Cl^-}$, is thus accompanied

with a critical level of acidity, $c^*_{H^+}$, above which no pit repassivation occurs. The critical chloride–hydrogen ion concentration, $c^*_{H^+}(c^*_{Cl^-})$, will then determine the pit stability. Pitting corrosion continues occurring if $c_{H^+}(c_{Cl^-}) \geq c^*_{H^+}(c^*_{Cl^-})$, but repassivation occurs if $c_{H^+}(c_{Cl^-}) < c^*_{H^+}(c^*_{Cl^-})$.

Metallic passivity in general occurs beyond the passivation potential, $E_P$, which becomes more positive with increasing solution acidity as mentioned earlier. It may hence be accepted that even for the critically acidified pit solution, the passivation potential may occur, which we call the critical *passivation–depassivation potential*, $E^*_P$, for the acidified pit solution. The $E^*_P$ obviously stands much more positive than the normal passivation potential, $E_P$, for the solution outside the pit. It appears, then, that as the repassivation potential, $E_R$, of the pit goes down more negative than the critical depassivation potential $E^*_P$, pit repassivation never occurs, and that pitting corrosion in the electropolishing mode turns to be the usual mode of active metal dissolution with the metal potential falling down into the range of the active state.

Figure 1.8 schematically shows that the pit-repassivation potential $E_R$ intersects with the critical depassivation potential $E^*_P$ at a certain pit radius, $r^*_{pit}$, which is the largest size of the pit that is repassivable. A corroding pit never repassivates if it grows greater than its largest repassivable size $r^*_{pit}$.

The foregoing discussion indicates that both the pit-repassivation potential $E_R$ and the critical depassivation potential $E^*_P$ play a primary role in the stability of pitting corrosion of metals. For pitting corrosion to occur, a pit embryo first breaks out at a potential in the range of passivity, where the metal surface remains passive except for the pit site. As the pit grows in size, its repassivation

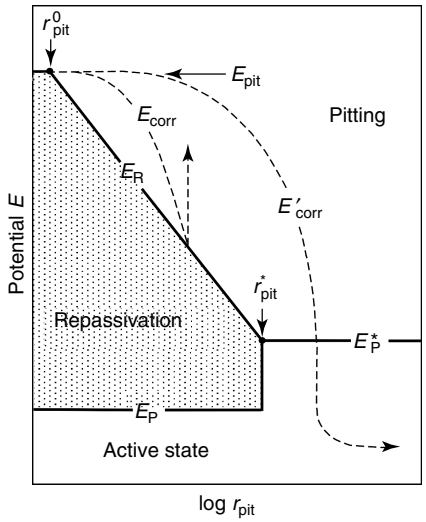


**Figure 1.8** Schematic potential–size curves for metallic pitting and pit repassivation: $r^*_{pit}$ is the maximum radius of repassivable pits, $r^0_{pit}$ is the critical size of pit embryos, and $E_{corr}$ is the corrosion potential of pitting metal.

potential $E_R$ goes down more negative, while the critical depassivation potential $E_P^*$ stays constant for the occluded pit solution at the critical chloride–hydrogen ion concentration, $c_{H^+}^*(c_{Cl^-}^*)$. It then appears that a corroding pit repassivates in the potential range between $E_R$ and $E_P^*$ as long as its repassivation potential is more positive than the critical depassivation potential ($E_R > E_P^*$). By contrast, a corroding pit never passivates if its repassivation potential goes down more negative than the critical depassivation potential ($E_R < E_P^*$), and consequently, no pit repassivation is expected to occur for the corrosion pit growing greater than the largest repassivable size, $r_{pit}^*$. The mode of local corrosion then changes from pitting corrosion to active pit corrosion, namely, from electropolishing to active dissolution.

The corrosion potential, as mentioned earlier, is controlled by the cathodic oxidant reduction. In the case of pitting corrosion, the cathodic reaction mainly occurs on the passive metal surface other than the pitting site. It is also known that the corrosion potential is made more positive and stable with increasing intensity and capacity of the oxidant reduction that supplies the cathodic current for corrosion. With the greater capacity of the cathodic reaction, the corrosion potential remains stable at relatively more positive potentials and the pit may be allowed to grow until its size exceeds the limiting value of repassivable pits, $r_{pit}^*$, before the potential falls down to its repassivation potential. Hence, no pit repassivation occurs as schematically shown in Figure 1.8. With the smaller capacity of the cathodic reaction, in contrast, the corrosion potential falls more steeply to the pit-repassivation potential before the pit grows over its limiting size of $r_{pit}^*$, and hence pit repassivation results.

We also note that the pitting potential is made more positive by lowering temperature until it reaches a certain temperature, called the *critical pitting temperature*, below which no pitting occurs [32]. For 316 stainless steels in sea water, the critical pitting temperature was about 30 °C [33]. Criterions of the temperature and potential for pitting corrosion all result from the stability requirement of pitting as described above.

### 1.4.2 Crevice Corrosion

Crevice corrosion is a type of localized corrosion that arises in structural crevices in the presence of chloride ions in aqueous solution. It normally occurs when the gap of a crevice is thinner than a certain width of the order of micrometers, which was estimated at 30–40 μm for usual stainless steel in acid solution [34]. The anodic metal dissolution in a crevice is usually coupled with the cathodic oxidant reduction that occurs outside the crevice, forming a local corrosion cell that involves the migration of hydrated ions through the crevice. For crevice corrosion to occur, a certain induction period is hence required to create a local corrosion cell between the inside and the outside of the crevice.

In general, crevice corrosion ceases growing in the potential range more negative than a certain critical potential, which we call the *crevice protection potential*, $E_{crev}$. Figure 1.9 schematically shows that the crevice is protected from corroding as the

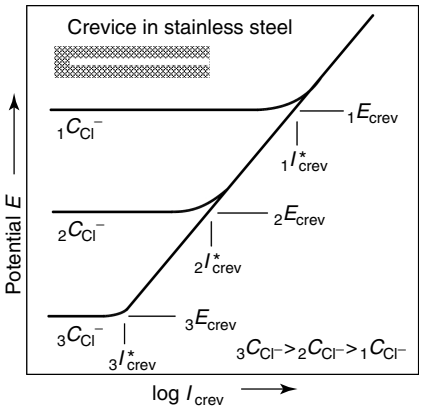


**Figure 1.9** Schematic potential–current curves for anodic dissolution of a cylindrical crevice in stainless steel in neutral solutions at three different chloride ion concentrations; $I_{crev}$ is the anodic crevice corrosion current, $c_{Cl^-}$ is the chloride ion concentration outside the crevice, $E_{crev}$ is the crevice protection potential, and $I^*_{crev}$ is the crevice corrosion current at $E_{crev}$ [34].

potential of the corroding crevice is made more negative than the crevice protection potential. The protection potential, $E_{crev}$, goes more negative with increasing chloride ion concentration, $c_{Cl^-}$ outside the crevice [34].

$$E_{crev} = E^0_{crev} - \alpha \log c_{Cl^-} \tag{1.23}$$

The threshold crevice corrosion current, $I^*_{crev}$, at the protection potential $E_{crev}$ is also found to be a linear function of the chloride ion concentration [34].

$$I^*_{crev} = I^0_{crev} - \beta c_{Cl^-}$$
$$\beta \propto \frac{1}{h_{crev}} \tag{1.24}$$

The coefficient, $\beta$, is found to be inversely proportional to the crevice depth, $h_{crev}$ [35].

It is the acidification of the occluded crevice solution that sets off crevice corrosion. The critical acidity that sets off crevice corrosion is equal to what is called the *passivation–depassivation pH*, above which the crevice passivates spontaneously and below which it remains in the active state. The passivation potential of the crevice metal at the passivation–depassivation pH provides the characteristic protection potential, $E^*_{crev}$, within the crevice. The actual potential that we measure involves an $IR$ drop, $\Delta E_{IR}$, caused by the ionic current through the crevice. From the kinetics of metal dissolution and mass transport, it is revealed that the crevice protection potential, $E_{crev}$, for a cylindrical crevice is a logarithmic function of the crevice depth, $h_{crev}$ [35, 36].

$$E_{crev} = E^*_{crev} + \Delta E_{IR} = a - b \log h_{crev} \tag{1.25}$$

We see that a linear relationship holds between the crevice protection potential, $E_{crev}$, and the logarithm of the crevice depth, $\log h_{crev}$, for a corrosion crevice of stainless steel in acid solution [35, 36].

No crevice corrosion occurs below a certain temperature called the *critical crevice corrosion temperature*, a situation which equates with the critical pitting temperature described earlier. The critical crevice temperature for stainless steel in seawater appears to be lower than the critical pitting temperature [37]. The crevice corrosion temperature has actually been used as a measure to evaluate metallic materials for their susceptibility to crevice corrosion.

### 1.4.3
### Potential–Dimension Diagram

From the foregoing discussion, we illustrate the stability of pitting and crevice corrosion in a potential–dimension diagram made up of the corrosion potential and the dimension of pitting and crevice corrosion, as schematically shown in Figure 1.10 [35, 36]. In general, as mentioned earlier, a corrosion pit first breaks out on the passivated surface of metals at the corrosion potential more positive than the pitting potential, $E_{pit}$, and it then grows in its size with a fall of the corrosion potential in the more negative direction.

If the supply of the cathodic current is insufficient for corrosion, the corrosion potential is rather unstable and readily falls down in the more negative direction with a relatively small rate of pit growth. Since the repassivation potential, $E_R$, of the small pit stands more positive than the critical depassivation potential $E_P^*$ for the pit solution, the falling corrosion potential reaches $E_R$ before arriving at $E_P^*$, and consequently, the small pit repassivates into the noncorrosive state. In contrast, if a sufficient supply of the cathodic current is available for pitting corrosion, the pit grows rather fast at relatively positive potentials until its size

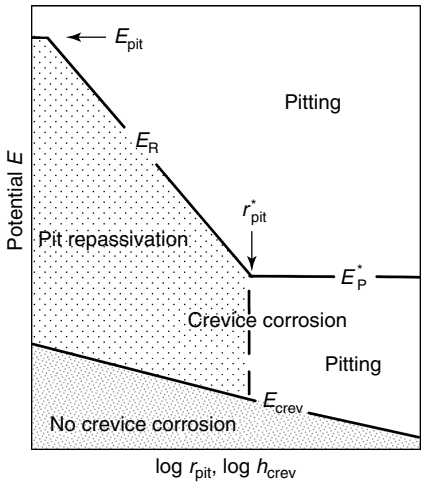


**Figure 1.10** Schematic potential–dimension diagram for localized corrosion of stainless steel in aqueous solution [35, 36].

exceeds the critical value, $r^*_{pit}$, beyond which no pit repassivation is expected to occur. The corrosion potential then gradually falls down to the critical depassivation potential, $E^*_P$, before reaching the pit-repassivation potential, $E_R$, and hence the pitting corrosion finally changes to the active mode of pit corrosion. We then see in the potential–dimension diagram that pitting corrosion progresses in the region in which the corrosion potential is more positive than both the pit-repassivation potential $E_R$ and the critical depassivation potential $E^*_P$, whereas it repassivates back to the passive state in the region in which the corrosion potential stands more negative than the pit-repassivation potential $E_R$ and more positive than the critical depassivation potential $E^*_P$.

In general, crevice corrosion breaks out in the region where the corrosion potential, $E_{corr}$, is more positive than the crevice protection potential, $E_{crev}$, at which the crevice solution is acidified to the passivation–depassivation pH of the crevice metal. We see in Figure 1.10 that no crevice corrosion is expected to break out in the region where the corrosion potential is more negative than the crevice protection potential. A corroding crevice may be made passive by shifting its corrosion potential into the region more negative than the crevice protection potential $E_{crev}$.

## 1.5
## Corrosion Rust

### 1.5.1
### Rust in Corrosion

Metallic corrosion in general produces metal ions oxidized in the hydrated form and then precipitates a mass of corrosion rust in the solid form. Hydrated metal ions are mostly hard Lewis acids and tend to combine with chemical species of hard Lewis bases such as hydroxide ions, chloride ions, sulfate ions, and phosphate ions to form somewhat covalent or ionic compounds in the soluble or insoluble state. Both soluble and insoluble corrosion products influence the subsequent progress in metallic corrosion, causing either corrosion acceleration or inhibition [38–40]. We examine in this chapter insoluble corrosion products, that is, corrosion rust.

Localized corrosion normally involves the transport of hydrated ions in the corrosion cell: anions migrate from the cathodic reaction site to the anodic reaction site, and cations migrate in the reverse direction. In the presence of a substantial mass of corrosion rust on the metal surface, the ionic migration occurs through the rust precipitate, and the occluded solution directly in contact with the metal under the rust may change its concentration in aggressive ions if the ions migrate selectively across the rust. The ion-selective nature of the rust, therefore, plays an influential role in the corrosion of rust-covered metals.

Corrosion rust in general is more or less ion selective, and its ion selectivity is determined by the fixed ionic charge in the more-or-less porous rust. The rust is anion selective if the fixed charge is positive, while it is cation selective if the fixed

charge is negative. Aluminum oxide is anion selective in neutral sodium chloride solution and turns to be cation selective in basic sodium hydroxide solution [41]. Oxides such as hydrous ferric oxide, nickel oxide, and chromic oxide are anion selective in neutral chloride solution [42–44]. The ion selectivity of corrosion rust is normally estimated in terms of the transference number, $\tau$, of migrating ions through the rust. It is found with a hydrous ferric oxide layer that $\tau_{Cl^-} = -0.94$ and $\tau_{Na^+} = 0.06$, indicating that ferric oxide is anion selective in neutral sodium chloride solution [45]. The transference number of water, $\tau_{H_2O}$, also estimates the osmotic flow of water through the rust [46].

Normally, metal hydroxides are anion selective in acidic solution and turns to be cation selective beyond a certain pH, called the *isoelectric point* $pH_{iso}$; $pH_{iso} = 10.3$ for ferric oxide, and $pH_{iso} = 5.8$ for ferric–ferrous oxide [47]. Because of its effect on the ionic fixed charge, the adsorption of multivalent ions exerts a significant role on the ion selectivity of hydrous metal oxides. We see, for instance, that hydrous ferric oxide that is anion selective in neutral chloride solution turns to be cation selective with the adsorption of multivalent anions such as divalent sulfate ions, divalent molybdate ions, and trivalent phosphate ions [44, 47].

Metallic corrosion, as mentioned earlier, requires not only ionic transfer and migration but also electronic transfer at the surface of metals and rust deposits. It appears that corrosion rust mostly falls in the category of electronic semiconductors, whose electronic energy band structure differs from that of metals. For metals, the Fermi level, $\varepsilon_F$, (the electrode potential, $E$,) is in the conduction band where electrons are freely mobile, whereas for semiconductors, the Fermi level, $\varepsilon_F$, is located in the forbidden band gap where no freely mobile electrons are allowed to be present. The cathodic reaction involving electron transfer, therefore, proceeds differently on the metal and on the semiconductor. Metallic corrosion receives, as a result, an influence from the electron-selective nature of the rust. It is also apparent that the electrode potential of the rust formed on the metal may be either more positive or more negative than the corrosion potential of the metal, depending on whether the rust is n-type or p-type. Normally, iron oxide and zinc oxide are n-type oxides, while nickel oxide and copper oxide are p-type oxides. The presence of semiconducting rust in contact with metals may have an electronic influence to a certain extent on the metallic corrosion. We will discuss in the following sections how the ionic and the electronic character of corrosion rust affect metallic corrosion.

### 1.5.2 Ion-Selective Rust

Let us suppose that anodic metal corrosion is in progress under an anion-selective rust layer in aqueous solution containing chloride ions, with the cathodic reaction occurring somewhere away from the anodic corrosion site. The anodic metal dissolution current in the local corrosion cell carries chloride ions from the outside solution through the corrosion rust layer into an occluded solution under the layer, as schematically shown in Figure 1.11. Accumulation of chloride ions in the occluded solution under the rust layer finally reaches a stationary level at which

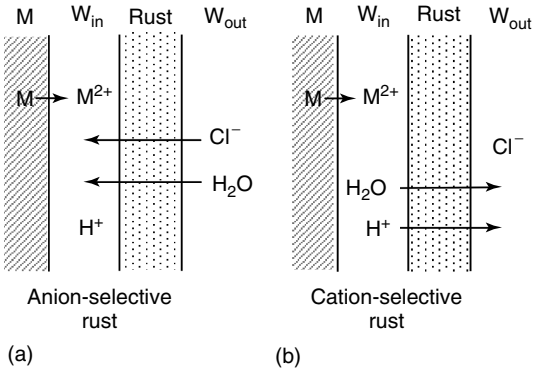


**Figure 1.11** Anion-selective and cation-selective rust layers on corroding metals: (a) anion-selective rust makes the occluded water acidify and (b) cation-selective rust makes the occluded water basify; M is the metal, $W_{in}$ is the occluded water under the rust, and $W_{out}$ is the water outside the rust.

the inward migration equals the outward diffusion of the ions. Furthermore, the inward chloride-ionic current carries water molecules by an electro-osmotic flow into the occluded solution. The final steady concentration of chloride ions under the anion-selective rust layer is thus determined by the ratio of the transference number, $\tau_{Cl^-}$, of chloride ions to the transport number, $\tau_{H_2O}$, of water molecules for the layer [48].

As the local chloride ion concentration increases under the anion-selective rust layer, the occluded solution acidifies and eventually accelerates the corrosion of the underlying metal. In order to prevent metallic corrosion due to the enriched chloride ions from occurring under the anion-selective rust, we need to make the rust less anion selective or turn it cation selective by some means such as the adsorption of multivalent anions on the rust, as mentioned earlier.

We next consider a precipitate of cation-selective rust that covers over the surface of corroding metal. The anodic ion transport carries no chloride ions inward through the rust layer, but mainly carries hydrated hydrogen ions (protons) migrating outward from the occluded solution into the outside solution. No accumulation of both chloride and hydrogen ions is thus expected to occur in the occluded solution, where the depression of hydrogen ions causes the basification of the solution and stimulates rust precipitation. Furthermore, the electro-osmotic outward water flow along with the hydrogen ion migration counteracts the inward water diffusion into the occluded solution. Dehydration of the occluded solution may thus occur, resulting in the depletion of water required for anodic metal dissolution, which may suppress the corrosion of the underlying metal.

Metallic corrosion sometimes produces a bipolar rust layer consisting of an anion-selective inner layer and a cation-selective outer layer. The bipolar rust layer may be realized by means of the adsorption of multivalent anions, which turns an outer rust layer cation selective on the inner anion-selective rust layer. The ionic bipolar layer, just like a p–n electronic junction that adjusts electronic

transport in semiconductors, rectifies the ionic current across the bipolar junction, suppressing in the anodic direction the ionic migration across the rust layer [44]. Furthermore, the high barrier for ionic transport generates at the bipolar junction a high electric field and makes the bipolar layer dehydrate into a layer of compact corrosion-resistive rust. We thus assume that the bipolar ion-selective rust layer is likely to inhibit metallic corrosion, bringing the metal into the passive state. It is an observed fact that pitting corrosion in stainless steel containing molybdenum is inhibited by the molybdate ion adsorption that makes an outer rust layer cation selective on the original, anion selective rust deposit [49, 50].

It is worth noting at the end that the ion-selective nature of corrosion rust remains valid as long as the concentration of migrating ions is comparable with or less than that of the fixed charge in the rust. If the rust is so coarsely porous that the migrating ion may receive little influence from the fixed charge, no ion-selective migration is expected to occur. In contrast, if the rust is so dense that no hydrated ions may penetrate into it, the normal solid-state diffusion of dehydrated ions will take over only under an extremely intense electric field.

### 1.5.3 Electron-Selective Rust

We suppose that metallic corrosion produces n-type semiconductor rust of metal oxides or hydroxides on the metal surface. The corrosion potential, $E_{corr}$, of an isolated metal is usually different from the electrode potential of an isolated semiconducting oxide of the metal. Semiconductor oxide in general sets its electrode potential at around its flat band potential, $E_{fb}$, where no space charge arises in the semiconductor. For most metals and their oxides in practical use, the flat-band potential of n-type oxides is more negative (cathodic) than the corrosion potential of the metals. The n-type rust oxide in contact with the metal consequently shifts the corrosion potential more negative to equate the Fermi level, $\varepsilon_F$, of the metal with that of the semiconductor oxide, thus giving rise to a space charge layer in the semiconductor oxide, as schematically shown in Figure 1.12. As a result of shifting the corrosion potential in the more negative direction, the n-type semiconductor rust appears to reduce the metallic corrosion, whose rate normally increases with the more positive potential. Furthermore, under the sunlight that injects photo-exited mobile holes (electron vacancies) in the valence band of electron energy levels in the semiconductor, the potential of the space charge layer is reduced in the semiconductor and the corrosion potential consequently shifts further in the more negative direction, resulting in a further decrease in the corrosion rate.

Metallic corrosion in the active state usually increases as the corrosion potential shifts in the positive (anodic) direction, and in the passive state also, pitting corrosion occurs at more positive potentials than the pit-initiation potential, $E_{pit}$. It is then advantageous for protecting metals from general and localized corrosion that the corrosion potential is made more negative by placing a mass of n-type semiconductor rust on the metal surface. It is also worth noting that for some n-type semiconductor oxides under photo-excitation, anodic water oxidation may

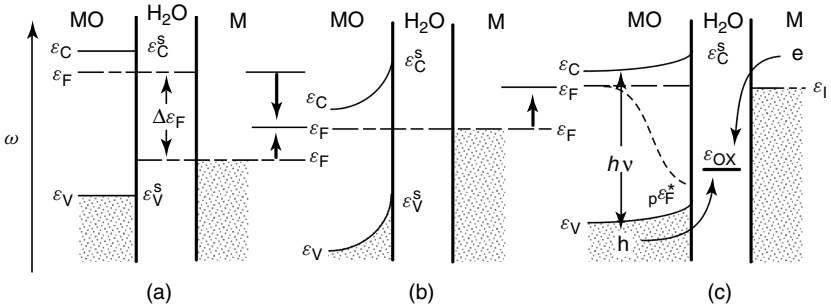


**Figure 1.12** Electron energy diagrams for metal and *n*-type oxide in contact with each other in aqueous solution: (a) prior to contact; (b) posterior to contact; and (c) under photo-excitation; M is the metal, MO is the metal oxide, $\varepsilon_F$ is the Fermi level, $\varepsilon_F^*$ is the quasi-Fermi level for photo-excited holes in oxide, $\varepsilon_C$ is the conduction band edge level, $\varepsilon_V$ is the valence band edge level, and $\varepsilon_{OX}$ is the Fermi level of oxygen electrode reaction.

occur producing gaseous oxygen even at potentials much more negative (cathodic) than the oxygen equilibrium potential. The anodic photo-excited water oxidation on the semiconductor, if coupled with cathodic oxidant reduction on the metal, may take over the anodic metal dissolution, and hence the metal may be protected from corrosion. We see that metallic copper and stainless steel were prevented from corrosion when they were brought into contact with n-type titanium oxide [50, 51]. The effectiveness of corrosion protection due to the n-type semiconductor, by its nature, depends on the ratio of the surface area of the metal to the semiconductor oxide. For stainless steel in contact with an n-type semiconductor of titanium oxide, effective corrosion inhibition was observed at the metal–oxide area ratio less than one tenth [51].

For most metal oxides and hydroxides of p-type semiconductors, in contrast, the flat band potential, $E_{fb}$, is more positive (anodic) than the corrosion potential, $E_{corr}$, of the metals. The corroding metal hence shifts its corrosion potential in the more positive (anodic) direction when it is brought in contact with a mass of p-type semiconductor oxide. Photo-excitation, in addition, further shifts the corrosion potential in the more positive direction. Metallic corrosion may then be accelerated if some p-type semiconductor rust is formed on the metal surface. In particular, pitting corrosion that occurs beyond the pit-initiation potential may break out in the presence of p-type semiconductor oxides on the metal. We also note that the photo-excitation of electrons from the valence band into the conduction band of p-type semiconductor oxide makes it thermodynamically possible for the cathodic hydrogen ion reduction to occur on the photo-excited p-type oxide even in the potential range much more positive (anodic) than the equilibrium hydrogen potential. It appears, as a result, that metallic copper, which suffers no corrosion without oxygen gas, may corrode even in the absence of gaseous oxygen, with the cathodic hydrogen ion reduction occurring on a mass of p-type copper oxides in contact with the metal under sunlight or radioactive rays. Hydrogen ion reduction involves radioexcited electrons in the conduction band of the p-type copper oxide.

### 1.5.4
### Redox Rust

Corrosion rust is occasionally subject to redox reactions on metals. We consider iron rust consisting of hydrous ferrous and ferric oxides, which are sensitive to reduction–oxidation reaction on the corroding iron surface.

$$Fe(OH)_3 + H^+_{aq} + e^-_M = Fe(OH)_2 + H_2O \quad (1.26)$$

For the redox reaction to occur, electrons and hydrogen ions will have to migrate through the hydrous oxide toward the reaction partners. In the cathodic reaction, hydrogen ions and electrons both migrate to ferric hydroxide to form ferrous hydroxide releasing water. The anodic reaction, inversely, draws both hydrogen ions and electrons out of ferrous hydroxide, with hydrogen ions migrating outward to the aqueous solution and electrons migrating inward to the metal surface. The reaction rate may thus be controlled by either hydrogen ion migration or electronic conduction in the redox rust.

The electrode potential of the ferric–ferrous redox reaction is normally more positive than the corrosion potential of metallic iron. The redox oxide in contact with the metal hence makes the corrosion potential of the metal more positive, and it also provides the metal corrosion with the cathodic reaction as follows:

$$Fe \rightarrow Fe^{2+}_{aq} + 2e^-_M \quad \text{anodic reaction} \quad (1.27)$$

$$2Fe(OH)_3 + 2H^+_{aq} + 2e^-_M \rightarrow 2Fe(OH)_2 + 2H_2O \quad \text{cathodic reaction} \quad (1.28)$$

The ferrous oxide thus reduced may then be oxidized by atmospheric gaseous oxygen to form ferric oxide on the metal.

$$2Fe(OH)_2 + 2H_2O \rightarrow 2Fe(OH)_3 + 2H^+_{aq} + 2e^-_M \quad \text{anodic reaction} \quad (1.29)$$

$$\frac{1}{2}O_2 + 2\,H^+_{aq} + 2e^-_M \rightarrow H_2O \quad \text{cathodic reaction} \quad (1.30)$$

The rate of the cathodic reduction of hydrous ferric oxide may be greater than the rate of the cathodic reduction of gaseous oxygen that normally occurs on the metal surface, hence the corrosion rate of metallic iron may be greater in the presence of ferric–ferrous redox oxide than in its absence on the metal surface. It is received understanding that the presence of redox rust may accelerate the corrosion of metals.

## 1.6
## Atmospheric Corrosion

### 1.6.1
### Atmospheric Corrosion Chemistry

Metallic iron and steel corrode in the moist atmosphere. The corrosion initially produces hydrated ferrous ions at the anode part and hydrated hydroxide ions at

the cathode part where air–oxygen is reduced to hydroxide ions, $OH^-_{aq}$. Hydrated ferrous ions in general arise in a variety of forms, such as $Fe^{2+}_{aq}$, $Fe(OH)^+_{aq}$, $Fe(OH)^0_{2,aq}$, and $Fe(OH)^-_{3,aq}$, depending on the pH of the solution. As the ferrous ion concentration exceeds its solubility limit, gel-like ferrous hydroxide, $Fe(OH)_{2,gel}$, precipitates out on the metal surface. According to thermodynamic calculations, gel-like ferrous hydroxide in pure water remains in equilibrium at pH 9.31 with its solubility at $1.27 \times 10^{-5}$ mol dm$^{-3}$ [52].

The hydrated ferrous ions initially formed in corrosion then air-oxidize into the solid precipitate of ferric hydroxide, $Fe(OH)_{3,solid}$.

$$4\left[Fe^{2+}_{aq} + 2OH^-_{aq}\right] + O_2 + 2H_2O \rightarrow 4Fe(OH)_{3,solid} \tag{1.31}$$

The term $\left[Fe^{2+}_{aq} + 2OH^-_{aq}\right]$ denotes the initial corrosion products at both anode and cathode parts. In the presence of a fair amount of gel-like ferrous hydroxide, $Fe(OH)_{2,gel}$, which maintains the solution at pH 9.31, the corrosion-produced ferrous ions in the hydrated form readily air-oxidize into the solid precipitate of ferric hydroxide, $Fe(OH)_{3,solid}$, and simultaneously, the pH of the solution changes to 7 with the solubility limit of ferric hydroxide at $1.20 \times 10^{-8}$ mol dm$^{-3}$ [52].

The ferric hydroxide precipitate thus formed gradually dehydrates into a mass of ferric oxyhydroxide.

$$Fe(OH)_{3,solid} \rightarrow FeOOH_{solid} + H_2O \tag{1.32}$$

Solid ferric oxyhydroxide $FeOOH_{solid}$ occurs in a variety of compounds such as $\alpha$-FeOOH, $\beta$-FeOOH, $\gamma$-FeOOH, and amorphous FeOOH. A mass of $\alpha$-FeOOH is the most stable, $\beta$-FeOOH is formed in the presence of chloride ions, $\gamma$-FeOOH is relatively stable, and an aggregate of amorphous FeOOH consists of extremely fine $\alpha$-FeOOH particles. The ferric oxyhydroxide thus formed in the early stage of corrosion tends to aggregate into a mass of dense solid precipitate in the pH range of 7–9.31, in which the oxyhydroxide retains almost no surface charge on it and hence readily coagulates into a mass of its precipitate [53]. The solubility limit of $\alpha$-FeOOH is $1.51 \times 10^{-13}$ mol dm$^{-3}$ and is much smaller than that of ferric hydroxide $Fe(OH)_{3,solid}$ [52].

Furthermore, the gel-like ferrous hydroxide of $Fe(OH)_{2,gel}$ formed in an early stage of corrosion air-oxidizes and dehydrates into magnetite, $Fe_3O_{4,solid}$, whose solubility limit is $1.10 \times 10^{-13}$ mol dm$^{-3}$ at pH 9.31 [52].

$$6Fe(OH)_{2,gel} + O_2 \rightarrow 2Fe_3O_{4,solid} + 6\ H_2O \tag{1.33}$$

The magnetite thus formed may be more or less electrochemically reactive, absorbing and desorbing hydrogen ions and electrons as well.

For metallic iron and steel containing alloying transition metal, M, atmospheric corrosion oxidizes the alloying metal into ferrite, $MFe_2O_4$, which then takes part in the rusting process. The ferrite may come out not only from the alloying elements but also from surface-coating substances on the metal.

$$2\ M(OH)_{2,solid} + 4Fe(OH)_{2,solid} + O_2 \rightarrow 2MFe_2O_{4,solid} + 4\ H_2O \tag{1.34}$$

The solubility of transition metal ferrites, such as $ZnFe_2O_4$, is as small as that of $\alpha$-FeOOH [52]. We see that, although occupying a minor concentration, transition metal ferrites play a significant role in developing anticorrosion rust in weathering steels as mentioned in the following sections [54].

Atmospheric corrosion normally proceeds in the cycles of wet and dry environments. According to what is called the *Evans model* [55], the anodic metal dissolution in the wet period is coupled with the cathodic reduction of ferric oxyhydroxide into reactive magnetite.

$$Fe \rightarrow Fe^{2+}_{aq} + 2e^{-}_{M} \quad \text{anodic reaction} \tag{1.35}$$

$$8FeOOH + Fe^{2+}_{aq} + 2e^{-}_{M} \rightarrow 3Fe_3O_4 + 4H_2O \quad \text{cathodic reduction} \tag{1.36}$$

In the dry stage, the reactive magnetite air-oxidizes into ferric oxyhydroxide.

$$4Fe_3O_4 + 8H_2O \rightarrow 12FeOOH + 4H^{+}_{aq} + 4e^{-}_{M} \quad \text{anodic oxidation} \tag{1.37}$$

$$O_2 + 2H_2O + 4H^{+}_{aq} + 4e^{-}_{M} \rightarrow 4H_2O \quad \text{cathodic reaction} \tag{1.38}$$

Combining the wet process with the dry process, we obtain the overall wet–dry corrosion process.

$$4Fe + 3O_2 + 2H_2O \rightarrow 4FeOOH \tag{1.39}$$

It is mainly iron oxyhydroxide rust that occurs in the atmospheric corrosion of metallic iron and steel.

In general, atmospheric corrosion frequently develops the rust into a multilayered structure composed of a variety of iron oxides, hydroxides, and oxyhydroxides mentioned above. It is also observed that as the rusting progresses the corrosive hydroxide rust gradually turns into the more corrosion-resistive rust consisting mainly of $\alpha$-FeOOH and amorphous FeOOH. The aged rust grows in an imbricate pattern, and the received wisdom is that the smaller imbricate scale provides weathering steels with more corrosion-resistive character.

### 1.6.2
### Weathering Steel Corrosion

Air pollutants such as chloride and sulfate, if present in the atmospheric moisture, penetrate the rust layer and create an anode channel for local corrosion. As the anodic metal dissolution progresses, the chloride and sulfate ions tend to accumulate in the anode channel where the aqueous solution acidifies. The concentrated ferrous chloride ions at 1 mol $dm^{-3}$ solution acidifies the solution at pH 4.75, where no ferrous hydroxide is allowed to precipitate in the solid state because of its solubility greater than 1 mol $dm^{-3}$. Hydrated ferrous chloride, $\left[Fe^{2+}_{aq} + 2Cl^{-}_{aq}\right]$, dissolved in local corrosion then gradually air-oxidizes and precipitates into ferric hydroxide rust in the anode channel, simultaneously producing hydrochloric acid $\left[H^{+}_{aq} + Cl^{-}_{aq}\right]$.

$$4\left[Fe^{2+}_{aq} + 2Cl^{-}_{aq}\right] + O_2 + 10H_2O \rightarrow 4Fe(OH)_{3,solid} + 8\left[H^{+}_{aq} + Cl^{-}_{aq}\right] \tag{1.40}$$

The acidified anode channel itself, however, still maintains a significant concentration of hydrated ferrous and ferric ions. These hydrated ions gradually leak out of the anode channel and air-oxidize into corrosion rust outside the anode channel. A model calculation estimates for the total concentration of corroded iron at 1 mol $dm^{-3}$ that air-oxidation finally gives rise to the solution that contains 0.590 mol $dm^{-3}$ of $Fe_{aq}^{+3}$ and 0.096 mol $dm^{-3}$ of $FeOH_{aq}^{+2}$ at the acidic level of pH 1.41 [52]. In the calculation, one-third of the corroded iron precipitates as gel-like ferric hydroxide, $Fe(OH)_{3,solid}$, in the anode channel at pH 1.41. Owing to its substantial surface charge in acidic solution, the gel-like ferric oxide assumes almost no aggregation into solid precipitates but disperses itself in the acidified anode channel, gradually dehydrating into $\beta$-FeOOH. The gel-like $\beta$-FeOOH then diffuses out forming a flowing mass of nonprotective yellow rust on the metal surface. The remaining two thirds of corroded iron remains in the form of soluble complexes of ferric ions and diffuses out of the anode channel to precipitate into several varieties of fresh corrosion rust in the neutral solution outside the aged rust layer.

In the anode channel containing acidified chloride ions and ferric ions, metallic iron corrodes with the cathodic oxidant reduction of hydrogen ions and ferric ions.

$$Fe + \left[2\,H_{aq}^{+} + 2Cl_{aq}^{-}\right] \rightarrow \left[Fe_{aq}^{2+} + 2Cl_{aq}^{-}\right] + H_2 \tag{1.41}$$

$$Fe + \left[2Fe_{aq}^{3+} + 6Cl_{aq}^{-}\right] \rightarrow \left[3Fe_{aq}^{2+} + 6Cl_{aq}^{-}\right] \tag{1.42}$$

The acidic corrosion reactions continue occurring as long as the anode channel keeps its solution sufficiently acidic.

Weathering steels are normally subject to cyclic wet–dry corrosion in the atmosphere. In the wet period, they corrode locally, producing yellow rust that flows out of the aged rust layers on the steels. In the dry period, on the other hand, the freshly formed rust dehydrates and air-oxidizes into a dense rust layer. The corrosion rust develops, as a result, into a multilayered structure successively consisting of dense and coarse rust layers formed in the dry and wet periods.

Long-term observations of atmospheric corrosion of steels show that a linear bilogarithmic relation holds between the corrosion weight loss or penetration, $w_{corr}$, and the time, $t$, of corrosion for 20–30 years [56, 57].

$$\begin{aligned} w_{corr} &= k_1 t^{k_2} \\ \log w_{corr} &= A + B \log t \end{aligned} \tag{1.43}$$

Parameters $k_1$, $k_2$, $A$, and $B$ are dependent on the type of steel materials and on the corrosion environments. No theoretical background has so far been made clear of Eq. (1.36), which, however, can be used to predict atmospheric corrosion for longer periods.

### 1.6.3 Anticorrosion Rust

It comes out of the foregoing discussion that the key point for weathering steel corrosion is to make the soluble product of ferrous ions air-oxidize as soon as possible into insoluble ferric hydroxide, which eventually turns to be anticorrosion rust on the metal surface. In general, the rate of air-oxidation of hydrated ferrous ions is much greater in neutral solution than in acid solution where no air oxidation of the ions virtually occurs. Once gel-like ferric hydroxide and ferrous hydroxide are formed in water, the solution remains around pH 7–9.31 where the air oxidation rate of ferrous ions is great. In the presence of chloride ions, however, the solution acidifies in the anode channel and hence reduces the rate of the air-oxidation of ferrous ions, eventually counteracting the formation of anticorrosion rust.

It is found that the presence of cupric ions, $Cu^{2+}$, and phosphate ions, $PO_4^{3-}$, catalytically accelerates the air-oxidation of ferrous ions even in acid solution [58]. Weathering steels usually contain copper and phosphorus as alloying elements, which dissolve in the form of hydrated ions. The dissolved cupric and phosphate ions increase the rate of the air oxidation of ferrous ions into solid ferric hydroxide in the acidified anode channel, and they thus contribute to the formation of anticorrosion rust.

For some reason not yet made clear, cupric ions $Cu^{2+}$ also influence the coagulation of hydroxide and prevent ferric hydroxide from crystallizing into coarse nonresistive aggregates [59, 60]. The rust then remains amorphous and grows into a dense, void-free barrier layer of anticorrosive rust. In general, transition metal ions such as $Ti_{aq}^{4+}$, $Co_{aq}^{2+}$, $Cr_{aq}^{3+}$, and $Ni_{aq}^{2+}$, which all come from alloying elements in weathering steels, are also found to catalyze the formation of amorphous iron rust [61, 62]. It is the received understanding that the amorphous rust of ferric oxyhydroxide is much more anticorrosive than the coarse crystalline oxide rust.

The ion-selective character of rust may also affect the corrosion of weathering steels. As mentioned earlier, the rust layer of cation-selective character prevents the occluded solution in the anode channel from being acidified and thus contributes to the formation of corrosion-resistive rust. The rust layer of anion-selective character, on the other hand, tends to make the anode channel acidify, thus retarding the formation of anticorrosion rust. It is, as mentioned earlier, the fixed charge on the inner surface of the rust that generates the ion-selective nature of the rust. The fixed charge depends on various factors such as adsorbed acid–base hydroxyl groups, nonstoichiometric surface composition, and specific adsorption of multivalent ions. In general, the surface charge of iron oxides and hydroxides is positive in the acidic range of water and negative in the basic range of water. The border pH, called the *isoelectric point* $pH_{iso}$, differs with different sorts of iron rust. It appears that the more acidic is the isoelectric point the more corrosion resistive is the rust. It is noted that the specific adsorption of multivalent anions such as $PO_4^{3-}$ and $CrO_{4,aq}^{2-}$, which come from alloying elements P and Cr in weathering steels, makes the isoelectric point pH, $pH_{iso}$, of the iron rust more acidic and hence contributes to the formation of anticorrosive rust layers on the steels.

## 1.7 Concluding Remarks

Corrosion science has made clear that metallic corrosion is in essence an electrochemical process combined with Lewis acid–base reactions at the interface between the metal and the environment, hence the corrosion potential plays a primary role in the process of corrosion. We have, however, a number of crucial issues to be studied to understand further the electrochemical and Lewis acid–base character of metallic corrosion at the molecular level.

In this chapter we have discussed metallic corrosion only under normal conditions. We note that corrosion also occurs under mechanical stresses leading to environmental cracking, stress corrosion cracking, erosion corrosion, and cavitation corrosion. Furthermore, materials other than metals, such as semiconductors, ionic solids, ceramics, and organic polymers, are also more or less all subject to corrosion [63].

## References


1. Evans, U.R. (1937) *Metallic Corrosion and Protection*, Edward Arnold, London.
2. Wagner, C. and Traud, W. (1938) Über die Deutung von Korrosionsvorgängen durch Überlagerung von elektrochemischen Teilvorgängen und über die Potentialbildung an Mischelektroden. *Z. Elektrochem.*, **44** (7), 391–402.
3. Wagner, C. (1974) Corrosion in aqueous solution and corrosion in gases at elevated temperature–analogies and disparities. *Werkst. Korros.*, **25** (3), 161–165.
4. Pourbaix, M. (1966) *Atlas of Electrochemical Equilibria in Aqueous Solutions*, Pergamon Press, Oxford.
5. Garreles, R.M. and Christ, C.L. (1965) *Solutions, Minerals and Equilibria*, Harper & Row, London, p. 172.
6. Kaesche, H. (1979) *Die Korrosion der Metalle*, 2 Auflage, Spring-Verlag, New York, p. 122.
7. Sato, N. (1989) Toward a more fundamental understanding of corrosion processes. *Corrosion*, **45**, 354–368.
8. Jensen, W.B. (1980) *The Lewis Acid-Base Concepts*, John Wiley & Sons, Inc., New York, pp. 112–336.
9. Okamoto, G., Shibata, T., and Sato, N. (1969) *Reports of Asahi Glass Foundation for Industrial Technology*, vol. 15, Asahi Glass Foundation for Industrial Technology, Tokyo, pp. 207–230.
10. Keir, J. (1790) *Philos . Trans.*, **80**, 259.
11. Sato, N. and Okamoto, G. (1981) Electrochemical passivation of Metals, in *Comprehensive Treatise of Electrochemistry*, vol. 4 (eds J.O'M.B. Bockris and R.E. White), Plenum Publishing Corporation, New York, London, pp. 193–245.
12. Sato, N. (1990) An Overview on the Passivity of Metals, in *Passivity of Metals Part I*, Corrosion Science, Vol. 31 (supplement) (eds N. Sato and K. Hashimoto), Pergamon Press, pp. 1–19.
13. Sato, N. (1976) Passivity of Iron, Nickel, and Cobalt – General Theory of Passivity, in *Passivity and its Breakdown on Iron and Iron Base Alloys* (eds R. Staehle and H. Okada), NACE, Houston, pp. 1–9.
14. Sato, N. (1982) Anodic breakdown of passive films on metals. *J. Electrochem. Soc.*, **129** (2), 255–260.
15. Sato, N. (2001) The stability and breakdown of passive oxide films on metals. *J. Indian Chem. Soc.*, **78**, 19–26.
16. Okamoto, G. and Sato, N. (1959) Self-passivation of nickel in aerated aqueous solution. *J. Jpn. Inst. Met.*, **23** (12), 725–728.

17. Takahashi, H., Fujimoto, F., Konno, H., and Nagayama, M. (1984) Distribution of aions and protons in oxide films formed anodically on aluminum in a phosphate solution. *J. Electrochem. Soc.*, **131** (8), 1856–1861.
18. Ohtsuka, T., Masuda, M., and Sato, N. (1985) Ellipsometric study of anodic oxide films on titanium in hydrochloric acid, sulfuric acid and phosphate solution. *J. Electrochem. Soc.*, **132** (4), 787–792.
19. Barr, T.L. (1979) An ESCA study of the termination of the passivation of elemental metals. *J. Phys. Chem.*, **82** (16), 1801–1810.
20. Fushimi, K. and Seo, M. (2001) Initiation of a local breakdown of passive film on iron due to chloride ions generated by a liquid-phase ion-gun for local breakdown. *J. Electrochem. Soc.*, **148** (11), B459–B456.
21. Fushimi, K., Azumi, K., and Seo, M. (2000) Use of a liquid-phase ion-gun for local breakdown of the passive film on iron. *J. Electrochem. Soc.*, **147** (2), 552–557.
22. Heusler, K.E. and Fisher, L. (1976) Kinetics of pit initiation at passive iron. *Werkst. Korros.*, **27** (8), 551–556.
23. Shibata, T. (1990) in *Passivity of Metals Part I*, Corrosion Science, Vol. 31 (supplement) (eds N. Sato and K. Hashimoto), pp. 413–423.
24. Sato, N. (1976) Stochastic process of chloride-pit generation in passive stainless steel. *J. Electrochem. Soc.*, **123** (8), 1197–1199.
25. Hisamatsu, Y., Yoshii, T., and Matsumura, Y. (1974) in *Localized Corrosion* (eds R.W. Staehle, B.F. Brown, J. Kruger, and A. Agrawal), NACE, Houston, TX, pp. 420–436.
26. Macdonald, D.D. (1992) The point defect model for the passive state. *J. Electrochem. Soc.*, **139** (12), 3434–3449.
27. Sato, N. (2001) *Proceedings of the 2nd International Conference on Environment Sensitive Cracking and Corrosion Damage, Hiroshima, October 29–November 3*, Japan Society Corrosion Engineering, pp. 49–54.
28. Brennert, C. (1937) Method for testing the resistance of stainless steels to local corrosive attack. *J. Iron Steel Inst.*, **135**, 101–112.
29. Hisamatsu, Y. (1976) in *Passivity and its Breakdown on Iron and Iron Base Alloys* (eds R.W. Staehle and H. Okada), NACE, Houston, TX, pp. 99–105.
30. Engell, H.J. and Storica, N.D. (1959) Untersuchungen über Lochfrass an passiven Elektroden aus unlegiertem Stahl in chloridenhaltiger Schwefelsaure. *Arch. Eisenhuttenwesen*, **30** (4), 239–248.
31. Sato, N. (1982) The stability of pitting dissolution of metals. *J. Electrochem. Soc.*, **129** (2), 260–264.
32. Laycock, H.J. and Newman, R.C. (1998) Temperature dependence of pitting potentals for austenitic stainless steels above their critical pitting temperature. *Corrosion Sci.*, **40** (6), 887–902.
33. Wallen, B. (2001) Critical Pitting Temperature of UNS S31600 in Different Sea Wateers, in *Marine Corrosion of Stainless Steels*, Pubication No. 33 (ed. D. Feron), European Federation of Corrosion, London, pp. 19–25.
34. Tsujikawa, S., Sono, Y., and Hisamatsu, Y. (1987) in *Corrosion Chemistry within Pits* (ed. A. Turnbull), National Physical Laboratory, London, p. 171.
35. Sato, N. (1995) The stability of localized corrosion. *Corrosion Sci.*, **37** (12), 1947–1967.
36. Sato, N. (2001) Potential-Dimension Diagram of Localized Corrosion, in *Marine Corrosion of Stainless Steels*, Publication No. 33 (ed. D. Feron), European Federation of Corrosion, London, pp. 185–201.
37. Steinsmo, U., Rogno, T., and Drugli, J.M. (2001) Recommended Practice for Selection, Quality Control and Use of High-Alloy Stainless Steels in Sea Water Systems, in *Marine Corrosion of Stainless Steels*, Publication No. 33 (ed. D. Feron), European Federation of Corrosion, London, pp. 115–123.
38. Sato, N. (2001) Ion-Selective Lust Layers and Passivation of Metals, in *Passivity of Metals and Semiconductors*, Proceedings 99-42 (eds B. Ives J.L. Luo, and J.R. Rodda), The Electrochemical Society, Inc., Pennington, pp. 281–287.

39. Sato, N. (2002) Surface oxide films affecting metallic corrosion. *Corrosion Sci. Technol.*, **31** (4), 262–274.
40. Sato, N. (1987) Some concepts of corrosion fundamentals. *Corrosion Sci.*, **27** (5), 354–368.
41. Huber, K. (1955) Über anodisch erzeugte Silberbromidschichten. Ein Beitrag zur Frage nach der Struktur von Elektroden II, Art. *Z. Elektrochem.*, **59** (7/8), 693–696.
42. Suzuki, M., Masuko, N., and Hisamatsu, Y. (1971) Study on the rust layer on atmospheric corrosion resistant low alloy steels, part 4 behavior of electrolyte in rust. *Boshoku Gijutsu (Jpn. Corrosion Eng.)*, **20** (7), 319–324.
43. Yomura, Y., Sakashita, M., and Sato, N. (1979) Ion-selectivity in hydrated iron (II), (II-III), and (III) oxide precipitate membranes. *Boshoku Gijutsu (Jpn. Corrosion Eng.)*, **28** (2), 64–71.
44. Sakashita, M. and Sato, N. (1979) Ion-selectivity of precipitate films affecting passivation and corrosion of metals. *Corrosion*, **35** (8), 351–355.
45. Sakashita, M., Yomura, Y., and Sato, N. (1977) Ion-selectivity of hydrous iron (III) oxide precipitate membranes. *Denki Kagaku (Jpn. Electrochem.)*, **45** (3), 165–170.
46. Sakashita, M. and Sato, N. (1975) Water transference through nickel hydroxide precipitate membrane. *J. Electroanal. Chem.*, **62** (1), 127–134.
47. Sakashita, M. and Sato, N. (1977) The effect of molybdate anion on the ion-selectivity of hydrous ferric oxide films in chloride solutions. *Corrosion Sci.*, **17** (6), 473–486.
48. Sakashita, M., Shimakura, S., and Sato, N. (1984) *Proceedings 9th International Congress Metallic Corrosion*, vol. 1, National Research Council of Canada, pp. 126–131.
49. Clayton, C.R. and Lu, Y.C. (1989) A bipolar model of the passivity of stainless steels–III, the mechanism of $MoO_4^{2-}$ formation and incorporation. *Corrosion Sci.*, **29** (7), 881–898.
50. Yuan, J. and Tsujikawa, S. (1995) Characterization of sol-gel-derived $TiO_2$ coatings and their photoeffectson copper substrates. *J. Electrochem. Soc.*, **142** (10), 3444–3450.
51. Fujisawa, R. and Tsujikawa, S. (1995) *Mater. Sci. Forum*, **183–189**, 1076–1081.
52. Tamura, H. (2008) The role of rusts in corrosion and corrosion protection of iron and steel. *Corrosion Sci.*, **50**, 1872–1882.
53. Cornell, R.M. and Schwertmann, U. (1996) *The Iron Oxides*, Wiley-VCH Verlag GmbH, Weinheim, p. 224.
54. Tamura, H. and Matijevic, E. (1982) Precipitation of cobalt ferrites. *J. Colloid Interface Sci.*, **90** (1), 100–109.
55. Evans, U.R. (1969) Mechanism of rusting. *Corrosion Sci.*, **9** (12), 813–821.
56. Fukushima, T., Sato, N., Hisamatsu, Y., Matsushima, T., and Aoyama, Y. (1982) Atmospheric Corrosion Testing in Japan, in *Atmospheric Corrosion* (ed. W.H. Ailor), A Wiley-Interscience Publication, John Wiley & Sons, Inc., New York, London, pp. 841–872.
57. Pourbaix, M. (1982) in *Atmospheric Corrosion* (ed. W.H. Ailor), A Wiley-Interscience Publication, John Wiley & Sons, Inc., New York, London, pp. 107–121.
58. Tamura, H., Goto, K., and Nagayama, M. (1976) Effect of anions on the oxygenation of ferrous ion in neutral solutions. *J. Inorg. Nucl. Chem.*, **38** (1), 113–117.
59. Furuichi, R., Sato, N., and Okamoto, G. (1969) Reactivity of hydrous ferric oxide containing metallic cations. *Chimia*, **23** (12), 455–465.
60. Suzuki, I., Hisamatsu, Y., and Masuko, N. (1980) Nature of atmospheric rust on iron. *J. Electrochem. Soc.*, **127** (10), 2210–2215.
61. Ishikawa, T., Uemo, T., Yasukawa, A., Kandori, K., Nakayama, T., and Tsubota, T. (2003) Influence of metal ions on the structure of poorly crystallized iron oxide rusts. *Corrosion Sci.*, **45**, 1037–1045.
62. Ishikawa, T., Maeda, A., Kandori, K., and Tahara, A. (2006) Characterization of rust on Fe-Cr, Fe-Ni, and Fe-Cu

bimary alloys by fourier transform infrared and $N_2$ adsorption. *Corrosion*, **62**, 559–567.

**63.** Sato, N. (2010) Fundamental Aspects of Corrosion of Metals and Semiconductors, in *Electrocatalysis: Computational, Experimental, and Industrial Aspects*, Surfactant Science Series, Vol. 149, Chapter 22 (ed. C.F. Zinola), CRC Press, Taylor & Francis Book, Inc., pp. 531–588.